Theor Chem Acc (2011) 130:871–881
DOI 10.1007/s00214-011-1032-7

REGULAR ARTICLE

Theoretical study of formation of ion pairs in $(NH_3{\cdot}HCl)(H_2O)_6$ and $(NH_3{\cdot}HF)(H_2O)_6$

Roger L. DeKock · Benjamin M. Brandsen · John R. Strikwerda

Received: 13 July 2011 / Accepted: 29 August 2011 / Published online: 25 September 2011

Abstract We have performed theoretical studies on sixteen molecular cubes for both $(NH_3{\cdot}HCl)(H_2O)_6$ and $(NH_3{\cdot}HF)(H_2O)_6$. We use an empirical gauge, based upon the N–H and H–X bond lengths, to categorize the degree to which the cubes are neutral adduct or ion pair in character. On this basis, we describe all sixteen cubes of the former as highly ionized, but only five of the latter as greater than 85% ionic in character. Addition of one or two bridging water molecules to form $(NH_3{\cdot}HF)(H_2O)_7$ or $(NH_3{\cdot}HF)(H_2O)_8$ raises the percent ionic character to greater than 85% for these systems. The relative energy of the cubes can be categorized based on simple chemical principles. The computed vibrational frequency corresponding to the proton stretch in the N–H–F framework shows the highest degree of redshifting for systems near 50% ion-pair character. Molecular cubes close to neutral adduct or to ion-pair character show less redshifting of this vibrational motion.

Keywords Hydrogen bonding · Density functional theory · Clusters · Ion pairs

Dedicated to Professor Akira Imamura on the occasion of his 77th birthday and published as part of the Imamura Festschrift Issue.

Electronic supplementary material The online version of this article (doi:10.1007/s00214-011-1032-7) contains supplementary material, which is available to authorized users.

R. L. DeKock (✉) · B. M. Brandsen · J. R. Strikwerda
Department of Chemistry and Biochemistry, Calvin College, 1726 Knollcrest Circle SE, Grand Rapids, MI 49546-4403, USA
e-mail: dekock@calvin.edu

1 Introduction

The importance of hydrogen bonding in chemistry cannot be overstated. One way to gauge its importance is to examine the number of monographs devoted to the topic. We list just five of them here [1–5]; two of these are devoted to computational/theoretical aspects of hydrogen bonding [1, 4]. In other literature, a recent "Frontiers Article" summarizes our knowledge of the hydrogen bond from a theoretical and experimental perspective [6]. A recent paper has examined both the infrared spectra and theoretical structures of $HCl(H_2O)_n$, where $n = 1$–3 [7]. Experimentalists and theoreticians probe the smallest number of water molecules needed to assist in ion-pair formation, as in $HCl(H_2O)_4$ [8, 9]. However, even for this relatively simple system, questions have arisen about the interpretation of the experimental infrared spectrum [10]. A theoretical study [11] of $HNO_3{\cdot}HCl{\cdot}H_2O$ has recently been reported, and connections drawn to atmospheric chemistry. Further related to atmospheric chemistry is the molecular dynamics work done by Anderson et al. [12] on clusters of $(H_2SO_4)_m{\cdot}Base{\cdot}(H_2O)_6$. Osuna, et al., have completed a density functional study of microsolvation of the alkali metal halides [13]. Molecular aspects of halide ion hydration have also been reviewed [14]. One of the interesting aspects of hydrogen bonding in aqueous systems is that "shuffling" of hydrogen atoms is at the heart of cooperativity among molecules and is responsible for proton solvation and proton mobility in aqueous systems [15].

The impetus for our work was provided by Belair and Francisco [16], who examined the electronic structure of the fourteen unique "ice cubes" of molecular formula $(H_2O)_8$ [17]. Additional motivation was provided by Kuo and Klein [18], who performed related studies on

molecular cubes of formula $HF(H_2O)_7$, which are isoelectronic to the ice cubes. Kuo and Klein used oriented graph theory to show that there were thirty-nine unique cubes for $HF(H_2O)_7$, with the HF hydrogen atom directed along one of the cube edges so that it could function as a proton donor to an adjacent water molecule. One such cube is shown in Fig. 1. These thirty-nine cubes result from differing topology of the hydrogen bond network. They found that seven of the cubes optimized to a more stable structure in which the HF molecule had ionized to form $H_3O^+F^-$. However, we note in passing that Kuo and Klein did not scan the F–H·····O coordinate to determine whether additional cubes would form ion pairs after passing over a low barrier.

For the NH_3·HX systems, we examine cubes of $(NH_3{\cdot}HCl)(H_2O)_6$ and $(NH_3{\cdot}HF)(H_2O)_6$ which have the H atom of HX internal to the cube, and one of the H atoms of NH_3 external to the cube. We also maintain the HX and the NH_3 adjacent to each other in the cube, with the hydrogen atom on HF directed toward the lone pair on NH_3, analogous to the work of Kuo and Klein. An example is shown in Fig. 2. Oriented graph theory shows that sixteen unique structures with configuration shown in Fig. 2 are possible [19]. The sixteen cubes are depicted in the supporting information. We have not done a global search of different conformations of the formula $(NH_3{\cdot}HX)(H_2O)_6$. Therefore, we cannot be sure that structures such as depicted in Fig. 2 represent the lowest energy conformation. However, we believe that these molecular cubes are the lowest energy conformation, based upon the fact that the most stable molecular structure of $(H_2O)_8$ is indeed the cube [17]. Chemical intuition would also favor this viewpoint.

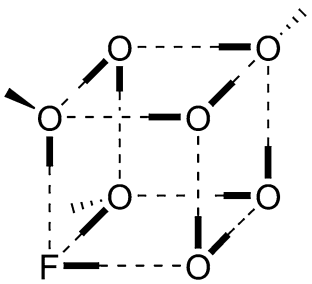

Fig. 1 Example of a cube structure with HF acting as a hydrogen bond donor

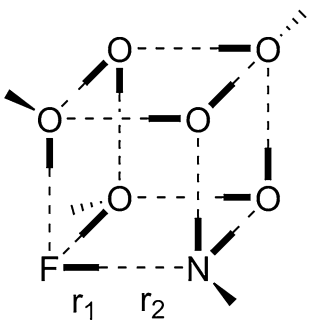

Fig. 2 Example of an $(NH_3{\cdot}HF)(H_2O)_6$ cube as studied here

Pertinent to our work is the earlier theoretical work on NH_3·HX [20] and on smaller clusters of $(NH_3{\cdot}HX)(H_2O)_n$ by Tao et al. [21–23]. The former work emphasized that coupling of harmonic vibrational frequencies necessitated solving the Schrödinger equation in two dimensions. That is, anharmonic effects were important to understand the experimental redshifting of the H–X stretching frequency brought about by hydrogen bonding in these dimers. In the latter work, Tao et al. observed a greater tendency for HCl to form ion pairs compared with HF, and the tendency for each to ionize increased as more water molecules were added.

To help us easily discern the tendency to ionize, we have developed [24] an empirical formula (see "Appendix") based upon the F–H bond length, r_1, and the H–N bond length, r_2, in the F–H–N framework, see Fig. 2. From a qualitative viewpoint, if r_1 is short and r_2 is long, the molecule will be mainly neutral molecule adduct; if the reverse is true, the molecule will be better described as an ion pair. Application of this empirical formula to the molecules studied by Tao is presented in Table 1. These results illustrate that, as stated above, HCl behaves quite differently from HF in regard to ion-pair formation and that more water molecules are capable of producing greater ion-pair character. Our results, see below, for the cubic molecules $(NH_3{\cdot}HX)(H_2O)_6$ show that this trend is borne out for these larger systems as well.

Our work has several objectives. (1) What will be the ion pair versus neutral adduct behavior of $(NH_3{\cdot}HF)(H_2O)_6$ and $(NH_3{\cdot}HCl)(H_2O)_6$? (2) Will there be two potential energy minima, one for ion pair and one for neutral, or will there be a single minimum? (3) Will there be a significant difference in the behavior of HF compared with HCl? (4) Can we understand the energy ranking of the sixteen cubes of $(NH_3{\cdot}HX)(H_2O)_6$ in simple chemical terms? (5) How is the percent ion-pair character altered by adding one or two additional water molecules to bridge the NH_3·HF framework of $(NH_3{\cdot}HF)(H_2O)_6$? (6) What trends do we observe in the computed vibrational frequency for the proton stretch in the N–H–F framework? Note that infrared spectroscopy is the main experimental technique used to

Table 1 Percent ion-pair contribution for various molecules of $(NH_3{\cdot}HX)(H_2O)_n$, B3LYP/aug-cc-pVTZ

	% Ion-pair HCl	% Ion-pair HF
NH_3·HX	6	5
$NH_3{\cdot}HX{\cdot}H_2O$	73	11
$NH_3{\cdot}HX{\cdot}2H_2O$	92	18

Table 2 Relative energies (kcal/mol) for the sixteen $(NH_3{\cdot}HF)(H_2O)_6$ molecules, optimized with the given methodology/basis set

	B3LYP/aug-cc-pVTZ	BP86/aug-cc-pVTZ	mPW1PW91/aug-cc-pVTZ	MP2/aug-cc-pVDZ
Cube 1	6.39	6.17	6.11	7.00
Cube 2	3.92	4.03	3.89	4.28
Cube 3	5.35	5.40	5.30	5.70
Cube 4	6.77	6.74	6.64	7.33
Cube 5	2.56	2.43	2.50	2.72
Cube 6	3.78	3.42	3.59	4.10
Cube 7	0	0	0	0
Cube 8	3.21	3.44	3.23	3.39
Cube 9	2.88	2.69	2.51	3.71
Cube 10	5.45	5.29	5.26	5.98
Cube 11	6.93	7.28	6.57	8.40
Cube 12	6.43	6.25	6.16	7.15
Cube 13	2.82	2.58	2.43	3.61
Cube 14	6.99	7.61	6.65	8.52
Cube 15	3.75	3.41	3.58	4.28
Cube 16	5.48	5.31	5.22	6.12

Relative energies are with respect to cube 7, the most stable structure

analyze molecular systems such as the title molecules. Hence, it will be useful to understand computed trends in the N–H–F proton stretching frequency.

2 Methodology

Initial geometry optimizations were performed at the B3LYP/cc-pVDZ level and B3LYP/aug-cc-pVDZ level. The B3LYP functional [25, 26] has been extensively applied to describe hydrogen bonding [27, 28] and has produced results comparable with MP2 [29–33]. The correlation consistent basis sets [34], especially those with augmented functions, have also been widely used to describe hydrogen bonding [18, 30, 35–38]. We also have employed MP2/aug-cc-pVDZ and the following density functionals/basis set: BP86/aug-cc-pVTZ and mPW1PW91/aug-cc-pVTZ [26, 39, 40].

The supporting information contains additional data regarding the relative energies and selected geometric parameters for the sixteen $NH_3{\cdot}HF(H_2O)_6$ cubes. As we will see in the results section, there is a strong correlation among relative energies and geometric parameters for the different methods and basis sets. In order to keep the paper appropriately concise for $NH_3{\cdot}HF(H_2O)_6$, we focus on one set of these results obtained at the B3LYP/aug-cc-pVTZ level.

We employ B3LYP/aug-cc-pVDZ for $NH_3{\cdot}HCl(H_2O)_6$. These molecules were already highly ionic at B3LYP/cc-pVDZ, and little change was observed upon going to B3LYP/aug-cc-pVDZ. Therefore, we did not pursue this to an even larger basis set. Later, we performed BP86/aug-cc-pVTZ on all sixteen cubes of $NH_3{\cdot}HCl(H_2O)_6$ (supporting information). This confirmed the high degree of ionization for these cubes.

Vibrational frequencies (harmonic) were computed for each geometry optimization. All vibrational frequencies were positive, indicating that (at least) a local minimum was obtained in each case. In all systems described, potential energy scans (e.g., increasing r_1, shortening r_2, Fig. 2) were performed to determine whether two local minima exist. None were found for these molecular systems. (see Figs. 8, 9 below, for examples.) The GAUSSIAN 03 and 09 program packages were employed for all our studies [41, 42]. We did not employ basis set superposition error corrections, since we are only interested in relative energies of similarly hydrogen-bonded networks, and not in the absolute value of the hydrogen bond energy.

Two papers have also appeared in the Imamura Festschrift issue that report on new and improved methodologies. One reports on a DFT method that includes long-range corrections (LC-DFT) [43], and another reports on multireference methods [44]. We believe that our methodology is adequate for the questions that we address with regard to ion-pair formation, but it may be of interest to apply methods such as these to our systems.

3 Results and discussion

3.1 Methodology and basis set effects for $(NH_3{\cdot}HF)(H_2O)_6$

As stated in the Methodology section, we employed a variety of different methodologies and basis sets to better ensure that our conclusions were not dependent upon these

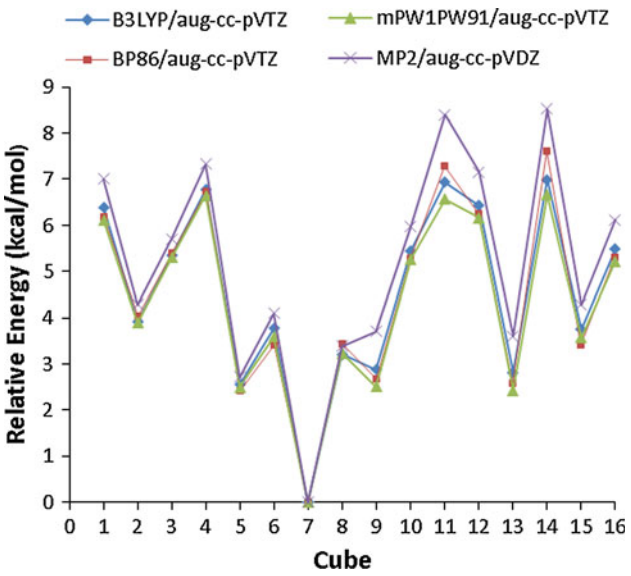

Fig. 3 Relative energy trends for the sixteen $(NH_3{\cdot}HF)(H_2O)_6$ molecules, optimized with the given methodology/basis set. Energies are relative to cube 7, the most stable structure

computational details. Table 2 shows the relative energies for all sixteen cubes of $(NH_3{\cdot}HF)(H_2O)_6$ obtained with four different methodologies/basis sets. These results are summarized graphically in Fig. 3. It is clear that there is a strong degree of correlation among these results.

We also examined the effect of methodology/basis set upon the geometric effects, presented as percent ion pair, within the N–H–F framework, Fig. 2. Full results of the raw geometric data are presented in the supplementary material. A graphical presentation is given in Fig. 4, which shows comparative results for MP2/aug-cc-pVDZ and B3LYP/aug-cc-pVTZ. This shows a very strong correlation for fourteen of the sixteen cubes. The remaining two cubes are neither strongly ionic nor strongly neutral in percent character, and hence the potential energy coordinate is broad for the N–H–F coordinate. Therefore, the lack of strong correlation here is not unexpected. This point is further discussed below in connection with Figs. 8 and 9.

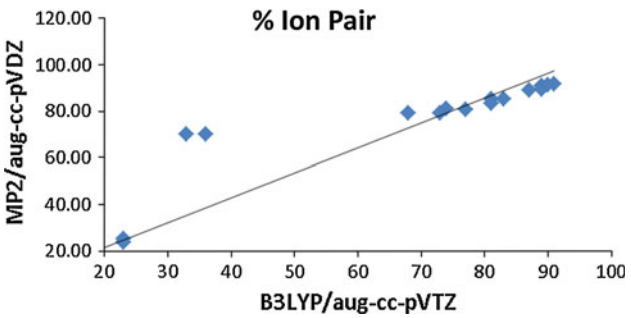

Fig. 4 Comparison of % ion-pair character at MP2/auc-cc-pVDZ and B3LYP/aug-cc-pVTZ

3.2 Structures, relative energies, and dipole moments of $(NH_3{\cdot}HCl)(H_2O)_6$

3.2.1 Structures

Table 3 shows the relative energies and pertinent bond lengths within the acid–base pair, percent contributions, and dipole moments for each of the sixteen structures for $(NH_3{\cdot}HCl)(H_2O)_6$. As seen in Table 3, the % ion-pair values range from 86 to 95%. The average N–H bond length is 1.07 Å (short), and the average H–Cl bond length is 1.96 Å (long). This high degree of percent ion-pair contribution was expected since we know from the theoretical literature [21–23] that one or two water molecules of hydration are capable of ionization of the $NH_3{\cdot}HCl$ adduct (Table 1). So it is not surprising that six water molecules, even though constrained by their cubic arrangement, are capable of inducing the $NH_3{\cdot}HCl$ adduct to form ion pairs.

3.2.2 Relative energies

Figure 5 illustrates the trend in relative energy among the sixteen molecular cubes. We observe four broad categories in this energy diagram. Figure 6 presents one molecular cube structure for each of these categories, ranked from low energy to high energy: cube 7, cube 6, cube 16, and cube 14. Referring to Fig. 6, a simple way to characterize the hydrogen bond topology is to look at the positions of the dangling hydrogen atoms. For the most stable structure, we see that the external hydrogen atoms are distributed in the most symmetric fashion possible. By contrast, for the least stable structure, they are distributed in the least symmetric way possible. The unstable nature of cubes with an asymmetric distribution of external hydrogen atoms is in good agreement with previous work that observes structures with nearest-neighbor external hydrogen atoms are more unstable than those without nearest-neighbor external hydrogen atoms [45, 46]. This arrangement of the dangling hydrogen atoms makes it easy to categorize the relative dipole moments shown in Table 3. For example, cube 7 is the most stable and has the lowest dipole moment. Cube 14 is least stable and has the highest dipole moment. But counting the arrangement of the dangling hydrogen atoms does not focus on the hydrogen bonds, which after all are the cause of the relative stability of the cubes. We take that up in the following two paragraphs.

To describe the pertinent geometric features that cause the energetic display shown in Fig. 5, we use the language of *donor* (D) and *acceptor* (A) for the hydrogen bond as employed by the Cambridge Structural Database. Namely, D–H·····A defines the meaning of the donor–acceptor relationship.

Table 3 $(NH_3{\cdot}HCl)(H_2O)_6$: N–H bond length (Å), Cl–H bond length (Å), % ion pair, relative energy (kcal/mol), and dipole moment for the sixteen unique structures at B3LYP/aug-cc-pVDZ

Structure	Cl–H length	N–H length	% Ion pair	Relative energy	μ (debye)
Cube 1	1.95	1.07	90.7	6.5	9.1
Cube 2	2.04	1.06	94.3	3.9	6.0
Cube 3	2.02	1.06	93.7	5.8	6.7
Cube 4	1.97	1.07	92.0	7.3	9.6
Cube 5	2.01	1.06	93.4	2.6	2.2
Cube 6	1.97	1.07	91.6	4.0	7.0
Cube 7	2.06	1.05	95.0	0.0	2.5
Cube 8	2.04	1.06	94.3	3.8	4.6
Cube 9	1.92	1.08	89.1	4.0	6.6
Cube 10	1.94	1.08	90.3	6.5	7.5
Cube 11	1.87	1.09	86.3	9.8	11.3
Cube 12	1.94	1.08	90.5	6.6	9.0
Cube 13	1.91	1.08	88.9	3.9	6.8
Cube 14	1.87	1.09	86.1	10.1	11.5
Cube 15	1.96	1.07	91.6	4.1	6.9
Cube 16	1.93	1.08	90.2	6.7	8.0

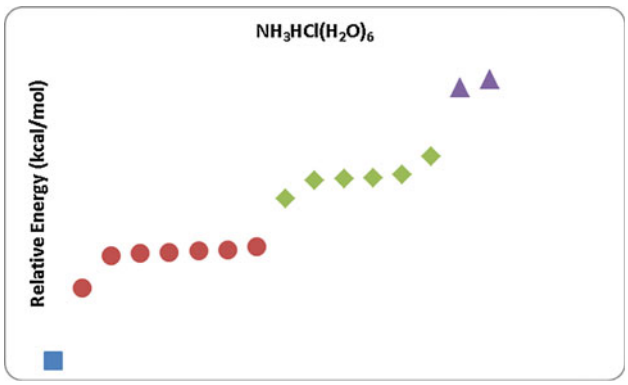

Fig. 5 Relative energies for the sixteen cubes formed by $NH_3{\cdot}HCl(H_2O)_6$

Belair and Francisco [16] explained the energy trend in the fourteen cubes of $(H_2O)_8$ in terms of the number of particular dimers within the cube that have the arrangement shown in Fig. 7. In these dimers, the donor water molecule has *one* dangling hydrogen atom, and the acceptor has *no* dangling hydrogen atoms (its two hydrogen atoms are internal to the cube). We will refer to these as B–F dimers, for Belair–Francisco. Our method of explaining the energy trend, Fig. 5, uses this particular arrangement as one of three aspects. The other two aspects deal with the ability to form strong hydrogen bonds to the ions Cl^- and NH_4^+. To form a strong hydrogen bond to the acceptor Cl^- requires that the *donor* water molecule exhibits one dangling hydrogen atom. Similarly, to form a strong hydrogen bond to the donor NH_4^+ requires that the *acceptor* water molecule has no dangling hydrogen atoms. These are in strict accord with the B–F water dimers. In fact, these "additions" to the B–F dimer rule are required because, unlike in their work with the water octamer, we observe the formation of ion pairs. We summarize these in Table 4 for each of the four cubes represented. Notice that the total number of these stabilizing features correlates well with the relative energy of these molecular cubes. That is, more stabilizing features result in a lower relative energy.

3.3 Structures, relative energies, and dipole moments of $(NH_3{\cdot}HF)(H_2O)_6$

Table 5 exhibits data for the sixteen cubes of $(NH_3{\cdot}HF)(H_2O)_6$ optimized with both the B3LYP/aug-cc-pVDZ and the B3LYP/aug-cc-pVTZ basis sets. The relative energies and dipole moments of the sixteen cubes can be categorized similarly to that for the corresponding HCl cubes, so we do not pursue that idea further. Rather, we focus on the bond lengths and the % ion-pair character. We then examine the most stable cube, cube 7, and compare it to the least stable cube, cube 14.

The N–H and H–F bond lengths are presented in Table 5, and each shows a wide range of variability between cubes. The N–H bond lengths range from a low of 1.08 Å to a high of 1.42 Å with the aug-cc-pVDZ basis set and from 1.08 to 1.45 Å with the aug-cc-pVTZ basis set. Likewise, the H–F bond lengths range from a low of 1.05 Å to a high of 1.49 Å with the aug-cc-pVDZ basis set, and from 1.04 to 1.48 Å with the aug-cc-pVTZ basis set. Table 5 also shows that the change in bond length due to the change in basis set is minor except for cubes 9 and 13, which we now discuss.

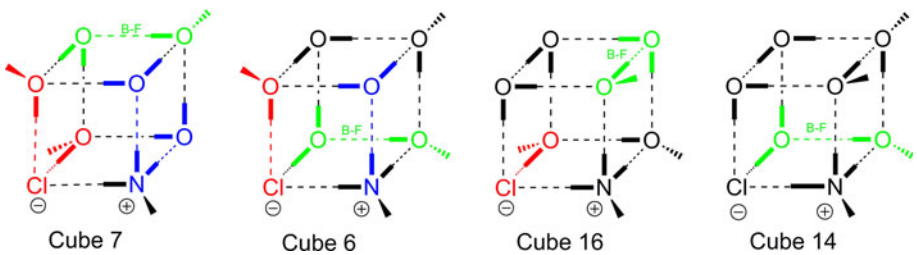

Fig. 6 Depictions of molecular cubes from each of the four categories of energy in Fig. 5, ranked in order. Cube 7 is lowest in energy, and cube 14 is highest

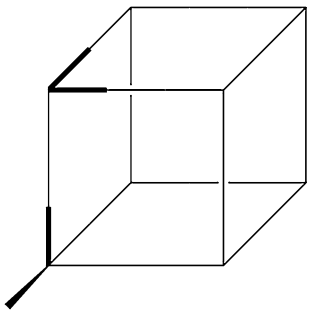

Fig. 7 Example of a B–F dimer structure as found within the larger cubic structure

Table 4 Important donor–acceptor relationship that categorize the relative energy of the cubes

Structure	B–F dimers	$Cl^{-}\cdot H_2O$ dimers[a]	$NH_4^{+}\cdot H_2O$ dimers[a]	Total	Energy[b]
Cube 7	1	2	2	5	0.0
Cube 6	1	1	1	3	4.0
Cube 16	1	1	0	2	8.0
Cube 14	1	0	0	1	11.5

[a] These dimers refer to those as described in the text

[b] In units of kcal/mol

Of all sixteen cubes, cubes 9 and 13 have the least *difference* ($\sim$0.1 Å) between the H–F and N–H bond lengths at the B3LYP/aug-cc-pVDZ level. That is, the H atom for these two cubes is nearly equidistant from both the N and F atoms. The cube has been "caught" in neither a neutral adduct structure nor an ion-pair structure. Generally, this means that it is in a portion of the potential energy curve along this internal coordinate that is relatively flat. For such situations, we can expect significant changes in geometry upon changing basis set, but little change in the relative energies. This situation is analogous to the much studied $NH_3\cdot HCl\cdot H_2O$ [21–23, 47–50]. In that case, the exact placement of the H atom between the N and the Cl atoms is very much dependent upon basis set and methodology. Again, there is a broad and flat potential energy surface along this internal coordinate.

We provide a specific example of this "flat" potential energy surface conundrum in Figs. 8 and 9. In this figure, we scan the N–H bond distance from 1.05 to 1.6 Å for cubes 9 and 10. (Cube 9 represents a flat potential energy surface for this coordinate, whereas cube 10 represents a stiffer potential.) The results are presented at the B3LYP/aug-cc-pVDZ level and MP2/aug-cc-pVDZ level. We observe little difference between the B3LYP and MP2 results. Further, we see that cube 9 has a very flat surface between 1.1 and 1.4 Å. As seen in Table 5, changing the basis set from aug-cc-pVDZ to aug-cc-pVTZ for cube 9 *decreases* the F–H bond distance from 1.24 to 1.08 Å, and correspondingly, the N–H distance *increases* from 1.20 to 1.36 Å. This change in geometry has a dramatic effect on the % ion-pair contribution as shown in Table 5. As we predicted, cube 9 with the flat potential energy surface is very sensitive to a change in basis set.

3.4 Comparison of $(NH_3\cdot HCl)(H_2O)_6$ with $(NH_3\cdot HF)(H_2O)_6$

The theoretical literature [21–23] on the $NH_3\cdot HF$ adduct indicates that a minimum of three water molecules of hydration are needed for ionization, indicating that one or two additional molecules of water are needed to induce

Table 5 $(NH_3\cdot HF)(H_2O)_6$: N–H bond length (Å), F–H bond length (Å), % ion pair, relative energy (kcal/mol), and dipole moment for the sixteen unique structures for B3LYP studies

Structure	F–H length	N–H length	% Ion pair	Relative energy	μ (debye)
Cube 1	1.31/1.25	1.15/1.19	77/68	6.7/6.4	6.8/6.6
Cube 2	1.47/1.45	1.09/1.09	90/89	4.1/3.9	4.0/4.0
Cube 3	1.45/1.43	1.09/1.09	89/89	5.5/5.4	6.3/6.3
Cube 4	1.38/1.37	1.11/1.12	85/83	7.0/6.8	8.4/8.3
Cube 5	1.43/1.42	1.10/1.10	88/87	2.7/2.6	1.0/1.1
Cube 6	1.37/1.34	1.12/1.13	83/81	3.9/3.8	5.2/5.1
Cube 7	1.49/1.48	1.08/1.08	92/91	0.0/0.0	1.3/1.3
Cube 8	1.47/1.46	1.08/1.09	91/90	3.3/3.2	5.6/5.7
Cube 9	1.24/1.08	1.20/1.36	66/33	3.5/2.9	4.3/3.4
Cube 10	1.33/1.29	1.14/1.16	79/74	5.7/5.5	6.9/6.8
Cube 11	1.06/1.04	1.41/1.44	28/23	7.9/6.9	7.8/7.7
Cube 12	1.32/1.28	1.14/1.17	78/73	6.7/6.4	6.9/6.7
Cube 13	1.24/1.09	1.19/1.35	67/36	3.4/2.8	4.4/3.3
Cube 14	1.05/1.04	1.42/1.45	26/23	8.0/7.0	8.1/7.9
Cube 15	1.37/1.34	1.12/1.13	83/81	4.0/3.8	5.1/5.0
Cube 16	1.33/1.31	1.14/1.15	79/77	5.8/5.5	7.4/7.3

The first value is for the aug-cc-pVDZ, and the second for the aug-cc-pVTZ basis

ionization compared with NH_3·HCl. These subtle differences between NH_3·HF and NH_3·HCl are also evident in comparison of our results in Tables 3 and 5. The simplest rubric to see this comparison is to examine the % ion-pair character in each of the tables. All sixteen of the $(NH_3·HCl)(H_2O)_6$ cubes are >85% ion-pair character. However, only five of the $(NH_3·HF)(H_2O)_6$ reach this level of ionization. We note by way of passing that there is a strong negative linear correlation between the percent ion-pair character and the N–H bond length. This is shown in the supporting information. It is an expected correlation if the N–F distance remains constant.

We can interpret the relative ability of ion-pair formation for $(NH_3·HF)(H_2O)_6$ versus $(NH_3·HCl)(H_2O)_6$ by employing the thermodynamic arguments of Cheung, Dixon, and Hershbach [51]. The essence of this argument is laid out in Table 6. We examine the energetics of formation of the ion-pair $NH_4^+X^-$ starting from the neutral species NH_3 and HX. This reaction is broken into several thermodynamic steps as shown in Table 6. The deprotonation reaction of HX is much more endothermic for HF than for HCl (370.5 vs. 332.5 kcal/mol). The proton affinity of NH_3 is a constant for both reactions (−204 kcal/mol). The last step in the thermodynamic cycle is the use of classical electrostatics to estimate the energy released upon bringing together the ions NH_4^+ and X^- to form an ion pair. We employ the average bond distance found between the N and Cl atoms in the sixteen cubes of $(NH_3·HCl)(H_2O)_6$, and also between the N and F atoms in the sixteen cubes of $(NH_3·HF)(H_2O)_6$. This allows us to obtain an estimate of the electrostatic attraction between the ions. Considering all of this, we find, as expected, that the formation of the ion pair is more endothermic in the case of $NH_4^+F^-$ than it is for $NH_4^+Cl^-$. Of course, neither of the models presented in Table 6 purports to incorporate the contribution from the water molecules that are assisting the formation of ion pairs through the cooperative nature of the hydrogen bonds. Furthermore, the classical treatment of the electrostatic attraction is a huge approximation compared with the quantum mechanical reality of the ions coming together. Nonetheless, this model gives us a crude understanding of the ability to form ion pairs in the two cases that we consider.

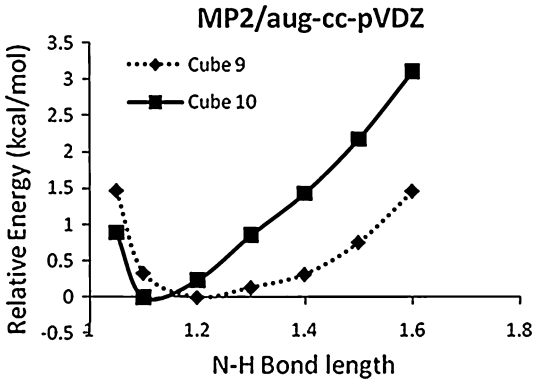

Fig. 8 Energy as a function of N–H bond length for cubes 9 and 10 at MP2/aug-cc-pVDZ

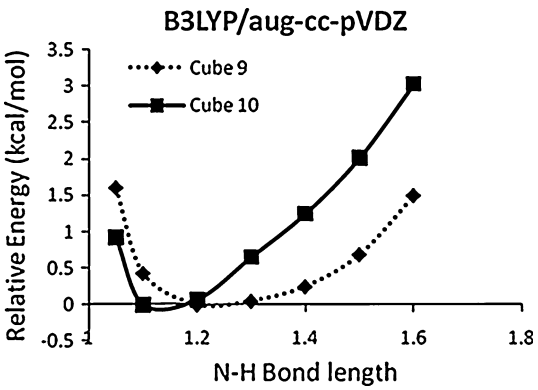

Fig. 9 Energy as a function of N–H bond length for cubes 9 and 10 at B3LYP/aug-cc-pVDZ

3.5 Correlation of vibrational frequency with geometry

To further understand the cooperative nature of hydrogen bonds, we examine the correlation of the computed harmonic vibrational frequency with geometry. We are interested in the computed vibrational frequency whose corresponding normal coordinate exhibits stretching motion of the H atom between the X and N atoms, and which has a large computed intensity. In Table 7, we present these frequencies, along with corresponding H–F and N–H bond lengths, and the % ion-pair character for the series of molecules HF, $HF·NH_3·(H_2O)_n$, for $n = 0$, 1, 2 and four representative cubes of the sixteen molecules for $n = 6$. The geometry data around the hydrogen bond are best depicted by use of the % ion-pair character rubric. We

Table 6 The thermodynamic steps (kcal/mol) used to compare relative ionization ability of NH_3·HF and NH_3·HCl

Process (gas phase)	X = F	Ref.	X = Cl	Ref.
$H \rightarrow H^+ + e^-$	313.6		313.6	
$X + e^- \rightarrow X^-$	−78.4	[52]	−83.3	[53]
$HX \rightarrow H + X$	135.3	[54]	102.2	[55]
$HX \rightarrow H^+ + X^-$	370.5		332.5	
$NH_3 + H^+ \rightarrow NH_4^+$	−204	[56]	−204	[56]
$NH_4^+ + X^- \rightarrow NH_4^+X^-$	−133.5[a]		−109.7[b]	
$NH_3 + HX \rightarrow NH_4^+X^-$	33.0		18.8	

[a] Based upon an electrostatic distance obtained from the average N–F distance in the sixteen cubes, 2.48 Å

[b] Based upon an electrostatic distance obtained from the average N–Cl distance in the sixteen cubes, 3.02 Å

Table 7 Vibrational frequency and associated information

Structure	N–H–F vibrational frequency/cm^{-1}	N–H bond length/Å	H–F bond length/Å	% Ion pair
HF	4,070	NA	0.92	0
NH_3·HF	3,217	1.67	0.96	5
NH_3·HF·H_2O	2,774	1.58	0.99	11
NH_3·HF·$(H_2O)_2$ (H_2O adj.)	2,311	1.49	1.02	28
NH_3·HF·$(H_2O)_2$ (H_2O not adj.)	2,065	1.45	1.035	22
NH_3·HF·$(H_2O)_6$ (Cube 14)	2,015	1.45	1.04	23
NH_3·HF·$(H_2O)_6$ (Cube 13)	1,377	1.35	1.09	36
NH_3·HF·$(H_2O)_6$ (Cube 1)	1,125	1.19	1.25	68
NH_3·HF·$(H_2O)_6$ (Cube 7)	2,487	1.08	1.48	91

See supplementary information for depictions of adducts with one and two water molecules of solvation

make use of this in Fig. 10 by graphing these stretching frequencies versus the % ion-pair character; this figure depicts all sixteen cubes for $n = 6$.

We note that the strong redshifting of the vibrational (hydrogen bond) frequency (853 cm^{-1}) has been documented in comparing HF and HF·NH_3 [1]. As seen in Table 7, addition of water molecules $n = 1$ and $n = 2$ further redshifts the vibrational frequency. We next look at the most stable structure of the sixteen cubes, namely the one that has the highest % ion-pair character, and its associated vibrational frequency, cube 7. We see that the frequency has increased above that for both of the molecules with $n = 2$. Of course, now the vibrational motion is better described as an ammonium ion in proximity to the fluoride ion rather than a neutral adduct HF·NH_3. We see that the frequency is still redshifted compared with free H–F, but not by as much as the molecules with $n = 2$. Table 7 also indicates data for three other representative molecular cubes, with % ion-pair character of 23, 36, and 68%. Figure 10 depicts the corresponding vibrational frequency for all of the molecules above, as well as the remainder of the sixteen molecular cubes. The vibrational frequency is redshifted the most when the H atom is "caught" most nearly in between the F and the N atoms. That is, the systems that are 35–70% ion pair in character are redshifted the most. We note in passing that there are instances wherein hydrogen bonding causes blueshifting of the vibrational frequency [57]. Figure 10 is reminiscent of Figure 6.19 in the monograph by Scheiner [1].

The data in Table 7 and Fig. 10 refer to harmonic vibrational frequencies. We know from earlier work on related systems [58, 59] that anharmonic effects are important to consider, if one wishes to relate directly to experiment. However, in our case, we are only comparing relative frequencies for related systems. We do not expect anharmonic corrections to change any of the discussion in the previous paragraph, although the absolute value of the frequencies will be lowered. In fact, we expect that anharmonic effects will be greatest for the systems near 50% ionic character, and therefore, the trend predicted in Fig. 10 will only be further enhanced.

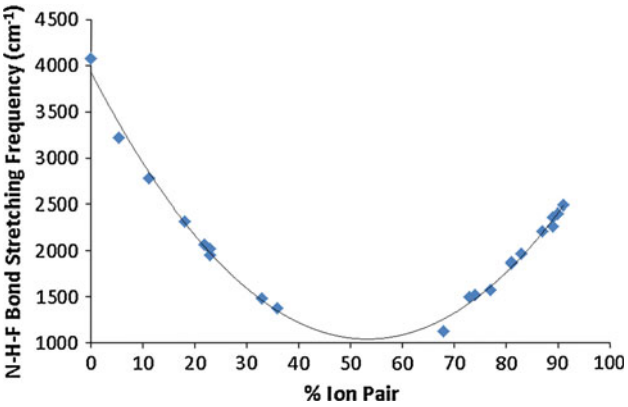

Fig. 10 Vibrational frequency versus ion-pair character

3.6 Addition of one and two water molecules to form (NH_3·HF)(H_2O)$_7$ and (NH_3·HF)(H_2O)$_8$

We added one and two additional water molecules to the NH_3·HF unit. An example is shown in Fig. 11 for cube 14 (least stable and least % ion-pair contribution). This work was done with B3LYP/aug-cc-pVDZ. All thirty-two cubes result in greater than 85% ion-pair character with these added waters of hydration. The resultant bond lengths and % ion-pair contributions are shown in the supporting information. For cube 14, the addition of two water molecules changes the % ion-pair character from ~23 to ~91%. The "active" hydrogen atom between F and N was caught in an unfavorable position due to the asymmetry in the hydrogen bond topology. Addition of two more water molecules evidently releases it from this unfavorable position and allows for migration to the N atom, forming an ion pair. By contrast, cube 7 was already ionized at 91% in its original cube form (Table 5). Addition of two water molecules increases this to 98%.

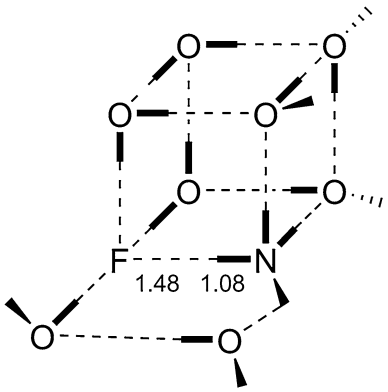

Fig. 11 Cube 14 with two bridging water molecules

4 Summary

Our work shows that $(NH_3{\cdot}HCl)(H_2O)_6$ exhibits a high degree of ion-pair character for all sixteen available cubes. The molecule $(NH_3{\cdot}HF)(H_2O)_6$ is less easily ionized and exhibits greater than 85% ion-pair character for only five of the sixteen possible cubes. One or two added waters of hydration result in all sixteen cubes having greater than 85% ion-pair character. The degree of ionization that we observe for $(NH_3{\cdot}HX)(H_2O)_6$ is in line with the earlier work of Tao et al., who already noted substantial ionization with fewer water molecules than six [21–23]. Our work is static, at 0 K, and could form the basis for molecular dynamics studies, such as in the case of $(H_2SO_4)_m{\cdot}$ Base$\cdot(H_2O)_6$ [12]. The relative energy of the cubes can be categorized based on simple chemical principles. The computed frequency corresponding to the N–H–F vibrational motion shows the highest degree of redshifting for systems near 50% ion-pair character. Molecular cubes close to neutral adduct or to ion-pair character show less redshifting of this vibrational motion.

Acknowledgments We gratefully acknowledge the Donors of the American Chemical Society Petroleum Research Fund for partial support of this research. We thank Laura A. Schipper and Stephanie C. Dykhouse for the preliminary work that they performed on this project. Computer hardware was provided by a Major Research Instrumentation Grant from the National Science Foundation, Award No. OCI-0722819.

Appendix

Empirical gauge of hydrogen bond versus ion-pair structure

We define a "reference" bond length and examine the relative difference between the reference bond length and that found in the molecule at hand. We use $NH_3{\cdot}HF$ and $NH_3{\cdot}HCl$ as our example molecules and employ our theoretical results to illustrate the method. Our empirical gauge relates the bond lengths $X \overset{r_1}{\leftrightarrow} H \overset{r_2}{\leftrightarrow} N$ to reference bond lengths. It is the distortion between the actual bond length and a reference bond length for each bond that measures the extent to which the structure is classified as a hydrogen bond adduct versus an ion-pair structure. In the following paragraph, we employ the aug-cc-pVDZ set for our theoretical results. Where experimental work is known, we place that in parentheses directly after the theoretical value.

The free molecule HF has a bond length of 0.926 Å (0.917 Å), and the corresponding value for HCl is 1.295 Å (1.274 Å). These computed values are labeled $r_{1\text{ref}}$ for HF and HCl, respectively. The second reference, $r_{2\text{ref}}$, is the N–H bond length in NH_4^+; we chose its value to be 1.0217 Å, [60].

We then define the following quantities that refer to ion-pair character and hydrogen bond character.

$$\text{i-p character} = \frac{r_1 - r_{1\text{ref}}}{r_{1\text{ref}}}$$

$$\text{h-b character} = \frac{r_2 - r_{2\text{ref}}}{r_{2\text{ref}}}$$

The experimental structure of $NH_3{\cdot}HF$ has not been reported, but the theoretical results are $r_1 = 0.966$ Å and $r_2 = 1.662$ Å. The corresponding theoretical values for $NH_3{\cdot}HCl$ are $r_1 = 1.370$ Å and $r_2 = 1.668$ Å. From these results, we obtain i-p character = 0.043 and h-b character = 0.583 for $NH_3{\cdot}HF$ and obtain i-p character = 0.058 and h-b character = 0.589 for $NH_3{\cdot}HCl$. In order to convert these into a percent contribution of each structure, we divide by a normalization factor, N, defined as the sum of these quantities.

$$N = \frac{r_1 - r_{1\text{ref}}}{r_{1\text{ref}}} + \frac{r_2 - r_{2\text{ref}}}{r_{2\text{ref}}}$$

The percent ion-pair character and percent hydrogen bond character for a given molecular structure are defined as follows:

$$\%\text{i-p} = \frac{r_1 - r_{1\text{ref}}}{N r_{1\text{ref}}} \times 100$$

$$\%\text{h-b} = \frac{r_2 - r_{2\text{ref}}}{N r_{2\text{ref}}} \times 100.$$

We obtain 93% h-b, 7% i-p for $NH_3{\cdot}HF$ and 91% h-b, 9% i-p for $NH_3{\cdot}HCl$. These results provide a quantitative way to report the amount of distortion that the acid undergoes upon bonding to the base. They confirm that the hydrogen bond is overwhelmingly an adduct pair, and not an ion pair. They show that $NH_3{\cdot}HCl$ is more "ionic" than $NH_3{\cdot}HF$, which makes qualitative sense, since chemists have many reasons to refer to HF as a weaker acid than HCl.

The empirical formula that we utilize here provides results that allow a quick empirical look at the nature of the

molecular adduct. Scheiner [1] provided an alternative view based upon a parameter he called ρ defined as $\rho = \Delta r(\mathrm{XH}) - \Delta r(\mathrm{NH})$.

References

1. Scheiner S (1997) Hydrogen bonding: a theoretical perspective. Oxford University Press, New York
2. Maréchal Y (2007) The hydrogen bond and the water molecule. Elsevier, New York
3. Jeffrey GA (1997) An introduction to hydrogen bonding. Oxford University Press, New York
4. Grabowski SJ (ed) (2006) Hydrogen bonding—new insights. Challenges and advances in computational chemistry and physics, vol 3. Springer, New York
5. Gilli G, Gilli P (2009) The nature of the hydrogen bond: outline of a comprehensive hydrogen bond theory. Oxford University Press, New York
6. Buckingham AD, Del Bene JE, McDowell SAC (2008) The hydrogen bond. Chem Phys Lett 463:1–10
7. Skvortsov D, Lee SJ, Choi MY, Vilesov AF (2009) J Phys Chem A 113(26):7360–7365
8. Gutberlet A, Schwaab G, Özgür B, Masia M, Kaczmarek A, Forbert H, Havenith M, Marx D (2009) Science 324:1545–1548
9. Re S, Osamura Y, Suzuki Y, Schaefer HF III (1998) Structures and stability. J Chem Phys 109:973–977
10. Morrison AM, Flynn SD, Liang T, Douberly GE (2010) J Phys Chem A 114(31):8090–8098
11. Gómez PC, Gálvez O, Escribano R (2009) Phys Chem Chem Phys 11:9710–9719
12. Anderson KE, Siepmann JI, McMurry PH, VandeVondele J (2008) J Am Chem Soc 130:14144–14147
13. Osuna S, Swart M, Baerends EJ, Bickelhaupt FM, Solà M (2009) Chem Phys Chem 10:2955–2965
14. Robertson WH, Johnson MA (2003) In: Leone SR, Alivisatos P, McDermott AE (eds) Annual review of physical chemistry, vol 54. Annual Reviews, Palo Alto, pp 173–213
15. Markovitch O, Agmon N (2007) J Phys Chem A 111(12): 2253–2256
16. Belair SD, Francisco JS (2003) Phys Rev A 67(6):063206
17. Gruenloh CJ, Carney JR, Arrington CA, Zwier TS, Fredericks SY, Jordan KD (1997) Science 276:1678–1681
18. Kuo J-L, Klein ML (2004) J Chem Phys 120:4690–4695
19. Stob MJ (1994) Private communication, Calvin College, July, 2007, Mathematica application of oriented graph theory. http://www.mathworld.wolfram.com/OrientedGraph. Harary, F. Graph Theory. Addison-Wesley, Reading, p 10
20. Del Bene JE, Jordan MJT (1998) J Chem Phys 108(8):3205
21. Cazar RA, Jamka AJ, Tao F-M (1998) J Phys Chem A 102:5117–5123
22. Snyder JA, Cazar RA, Jamka AJ, Tao F-M (1999) J Phys Chem A 103:7719–7724
23. Li R-J, Li Z-R, Wu D, Hao X-Y, Li Y, Wang B-Q, Tao F-M, Sun CC (2003) Chem Phys Lett 372:893–898
24. DeKock RL, Schipper LA, Dykhouse SC, Heeringa LP, Brandsen BM (2009) J Chem Educ 86(12):1459–1464
25. Lee C, Yang W, Parr RG (1988) Phys Rev B 37:785–789
26. Becke AD (1988) Phys Rev A 38:3098–3100
27. Lenz A, Ojamae L (2005) Phys Chem Chem Phys 7:1905–1911
28. Koch W, Holthausen MC (2001) A chemist's guide to density functional theory, 2nd edn. Wiley, New York, pp 213–232
29. Lee HM, Suh SB, Lee JY, Tarakeshwar P, Kim KS (2000) J Chem Phys 112:9759–9772
30. Silica MC, Muñoz-Caro C, Niño A (2005) ChemPhysChem 6:139–147
31. Lozynski M, Rusinska-Roszak D, Mack HJ (1998) J Phys Chem A 102:2899–2903
32. Odde S, Mhin BJ, Lee KH, Tarakeshwar P, Kim KS (2006) J Phys Chem A 110:7918–7924
33. Boese AD, Martin JML, Klopper WJ (2007) J Phys Chem A 111:11122–11133
34. Woon DE, Dunning TH Jr (1993) J Chem Phys 98:1358–1371
35. Christie RA, Jordan KD (2001) J Phys Chem A 105:7551–7558
36. Xantheas SS (2005) J Am Chem Soc 117:10373–10380
37. Xantheas SS, Dunning TH Jr (1993) J Chem Phys 99:8774–8792
38. Xantheas SS (1994) J Chem Phys 100:7523–7534
39. Perdew JP (1986) Phys Rev B 33:8822–8824
40. Adamo C, Barone V (1998) J Chem Phys 108(2):664
41. Frisch MJ, Trucks GW, Schlegel HB, Scuseria GE, Robb MA, Cheeseman JR, Montgomery Jr JA, Vreven T, Kudin KN, Burant JC, Millam JM, Iyengar SS, Tomasi J, Barone V, Mennucci B, Cossi M, Scalmani G, Rega N, Peterson GA, Nakatsuji H, Hada M, Ehara M, Toyota K, Fukuda R, Hasegawa J, Ishida M, Nakajima T, Honda Y, Kitao O, Nakai H, Klene M, Li X, Knox JE, Hratchian HP, Cross JB, Bakken V, Adamo C, Jaramillo J, Gomperts R, Stratmann RE, Yazyev O, Austin AJ, Cammi R, Pomelli C, Ochterski JW, Ayala PY, Morokuma K, Voth GA, Slavador P, Dannenberg JJ, Zakrzewski VG, Dapprich S, Daniels AD, Strain MC, Farkas O, Malick DK, Rabuck AD, Raghavachari K, Foresman JB, Ortiz JV, Cui Q, Baboul AG, Clifford S, Cioslowski J, Stefanov BB, Liu G, Liashenko A, Piskorz P, Komaromi I, Martin RL, Fox DJ, Keith T, Al-Laham MA, Peng CY, Nanayakkara A, Challacombe M, Gill PMW, Johnson B, Chen W, Wong MW, Gonzalez C, Pople JA (2003) Gaussian 03. Revision E.02 edn. Gaussian, Inc., Wallingford
42. Frisch MJ, Trucks GW, Schlegel HB, Scuseria GE, Robb MA, Cheeseman JR, Scalmani G, Barone V, Mennucci B, Petersson GA, Nakatsuji H, Caricato M, Li X, Hratchian HP, Izmaylov AF, Bloino J, Zheng G, Sonnenberg JL, Hada M, Ehara M, Toyota K, Fukuda R, Hasegawa J, Ishida M, Nakajima T, Honda Y, Kitao O, Nakai H, Vreven T, Montgomery JJA, Peralta JE, Ogliaro F, Bearpark M, Heyd JJ, Brothers E, Kudin KN, Staroverov VN, Kobayashi R, Normand J, Raghavachari K, Rendell A, Burant JC, Iyengar SS, Tomasi J, Cossi M, Rega N, Millam NJ, Klene M, Knox JE, Cross JB, Bakken V, Adamo C, Jaramillo J, Gomperts R, Stratmann RE, Yazyev O, Austin AJ, Cammi R, Pomelli C, Ochterski JW, Martin RL, Morokuma K, Zakrzewski VG, Voth GA, Salvador P, Dannenberg JJ, Dapprich S, Daniels AD, Farkas Ö, Foresman JB, Ortiz JV, Cioslowski J, Fox DJ (2009) Gaussian 09. Revision B.01 edn. Gaussian, Inc., Wallingford
43. Song J-W, Tsuneda T, Sato T, Hirao K (2011) Theor Chem Acc. http://www.dx.doi.org/10.1007/s00214-011-0997-6
44. Saito T, Nishihara S, Yamanaka S, Kitagawa Y, Kawakami T, Yamada S, Isobe H, Okumura M, Yamaguchi K (2011) Theor Chem Acc. http://www.dx.doi.org/10.1007/s00214-011-0914-z
45. Radhakrishnan TP, Herndon WC (1991) Graph theoretical analysis of water clusters. J Phys Chem 95(26):10609–10617
46. McDonald S, Ojamäe L, Singer SJ (1998) J Phys Chem A 102(17):2824–2832
47. Biczysko M, Latajka Z (1999) Chem Phys Lett 313(1–2): 366–373
48. Barnes AJ, Latajka Z, Biczysko M (2002) J Mol Struct 614(1–3):11–21
49. Abkowicz-Bienko A, Biczysko M, Latajka Z (2000) Comput Chem 24(3–4):303–309
50. Li R-J, Li Z-R, Wu D, Chen W, Li Y, Wang B-Q, Sun C–C (2005) J Phys Chem A 109(4):629–634
51. Cheung JT, Dixon DA, Herschbach DR (1988) J Phys Chem 92(9):2536–2541

52. Blondel C, Delsart C, Goldfarb F (2001) J Phys B Atomic Mol Optical Phys 34(9):L281–L288
53. Berzinsh U, Gustafsson M, Hanstorp D, Klinkmüller A, Ljungblad U, Mårtensson-Pendrill AM (1995) Phys Rev A 51(1): 231–238
54. Di Lonardo G, Douglas AE (1973) Can J Phys 51(4):434–445
55. Michel M, Korolkov MV, Weitzel K-M (2002) Phys Chem Chem Phys 4(17):4083–4086
56. Hunter EPL, Lias SG (1998) J Phys Chem Ref Data 27(3):413
57. Solimannejad M, Scheiner S (2007) J Phys Chem A 111:4431–4435
58. Gardenier GH, Johnson MA, McCoy AB (2009) J Phys Chem A 113(16):4772–4779
59. Soloveichik PO, Donnell BA, Lester MI, Francisco JS, McCoy AB (2010) J Phys Chem A 114(3):1529–1538
60. Dixon DA, Feller D, Peterson KA (2001) J Chem Phys 115(6):2576